Prediction model for the diffusion length in silicon-based solar cells

Cheknane A[1,†] and Benouaz T[2]

(1 Laboratoire d'Etude et Développement des Matériaux Semiconducteurs et Diélectrques, Université Amar Telidji de Laghouat, BP 37G, Laghouat 03000, Algérie)

(2 Laboratoire de Modélisation, Université Abou BakarBelkaid de Tlemcen Algérie)

Abstract: A novel approach to compute diffusion lengths in solar cells is presented. Thus, a simulation is done; it aims to give computational support to the general development of a neural networks (NNs), which is a very powerful predictive modelling technique used to predict the diffusion length in mono-crystalline silicon solar cells. Furthermore, the computation of the diffusion length and the comparison with measurement data, using the infrared injection method, are presented and discussed.

Key words: diffusion length; minority-carrier lifetime; infrared injection; solar cell; prediction; modelling
DOI: 10.1088/1674-4926/30/7/072001 **EEACC:** 2500

1. Introduction

The minority carrier diffusion length is one of the most important parameters to characterize the quality of silicon solar cells, because it provides a direct prediction of the conversion efficiency in silicon solar cells[1, 2].

As already known, the diffusion length represents the average distance an electron can travel before recombining. The diffusion constant of the minority carriers $D_{\rm n}$, the more interesting parameter in photovoltaics, is rather hard to detect[3].

This paper presents a comparative study of the two methods applied to silicon solar cells in determining diffusion lengths. The experimental technique consists of an infrared injection method where the infrared light was obtained by filtering light from a high-intensity xenon source; the computing method is based on a modelling technique using a neural network.

2. Theory

Under short-circuit conditions, the junction acts as a sink for minority carriers; hence[3],

$$n|_0 = 0. \tag{1}$$

Conditions at the back can be characterized by the general relationship:

$$D\left.\frac{{\rm d}n}{{\rm d}x}\right|_{\rm w} = -V_{\rm s} n|_{\rm w}\,. \tag{2}$$

The parameter $V_{\rm s}$, the surface recombination velocity, is a measure of the recombination rate within the surface region, while D is the minority-carrier diffusion constant. For extreme values of $V_{\rm s}$, Equation (2) reduces to

$$\begin{cases} n|_w = 0, & V_{\rm s} \to \infty, \\ \left.\dfrac{{\rm d}n}{{\rm d}x}\right|_{\rm w}, & V_{\rm s} \to 0. \end{cases} \tag{3}$$

The first condition applies to the case of strong recombination at the back, while the second condition applies to the case of no recombination.

The steady-state distribution of minority carriers can be represented by these boundary conditions and

$$D\frac{{\rm d}^2 n}{{\rm d}x^2} - \frac{n}{\tau_{\rm b}} = g, \tag{4}$$

where $\tau_{\rm b}$ is the minority lifetime, D is the minority-carrier diffusion constant and g is the minority-carrier generation rate.

Given a solution $n(x)$ to Eq. (4), one can compute the short-circuit current density $J_{\rm sh}$ using

$$J_{\rm sh} = qD\left.\frac{{\rm d}n}{{\rm d}x}\right|_0. \tag{5}$$

***Infrared injection**

When electron–hole pairs are generated by monochromatic light[4, 5], the generation profile has the form:

$$g_{\rm v} = F_0 \alpha \exp(-\alpha x), \tag{6}$$

where F_0 is the photon flux density at the junction and α is the optical absorption coefficient.

Referring to Eq. (4), the boundary conditions

$$n|_{x=0} = 0 \tag{7}$$

and

$$D\left.\frac{{\rm d}n}{{\rm d}x}\right|_{x=w} = -V_{\rm s} n|_{x=w} \tag{8}$$

taken from Eqs. (1) and (2), respectively, are of interest.

In the case of monochromatic infrared light, the generation profile is given by Eq. (1). The minority-carrier distribution becomes

† Corresponding author. Email: cheknanali@yahoo.com
Received 17 February 2009

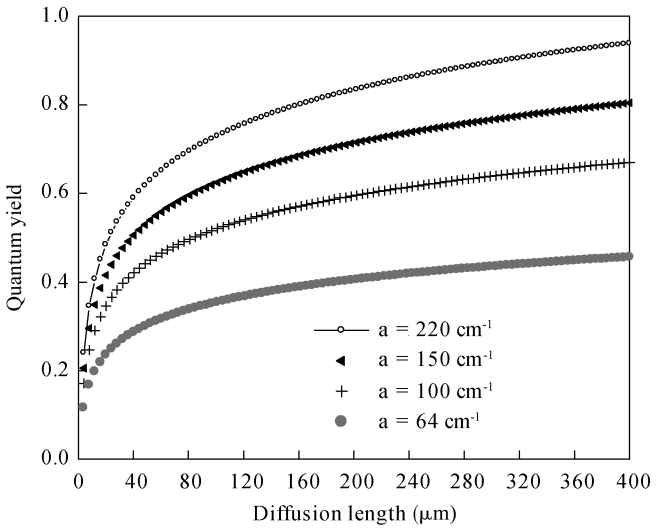

Fig. 1. Quantum yield as a function of minority-carrier diffusion length for several coefficients.

$$n = \frac{L^2}{D}\frac{\alpha F_0}{1-\alpha^2 L^2}\left\{\sinh\left(\frac{x}{L}\right)\left\{D\left[\exp\left(-w/L\right) - L\exp\left(-\alpha w\right)\right] + LV_{\rm s}\left[\exp\left(-w/L\right) - \exp\left(-\alpha w\right)\right]\right\}\left[LV_{\rm s}\sinh\left(w/L\right) - D\cosh\left(w/L\right)\right]^{-1} + \exp\left(-\alpha x\right) - \exp\left(-x/L\right)\right\}, \tag{9}$$

where L is the diffusion length, defined by

$$L = \sqrt{D\tau}. \tag{10}$$

Using Eq. (8), the expression of the current density J becomes

$$J = qD\left.\frac{{\rm d}n}{{\rm d}x}\right|_{x=0}. \tag{11}$$

The results for extreme values of $V_{\rm s}$ are

$$J = J_\infty\left(1 - \frac{\exp(-\alpha w) - \exp(-w/L)}{(1-\alpha L)\sinh(w/L)}\right),\ V_{\rm s}\to\infty, \tag{12}$$

$$J = J_\infty\left(1 - \frac{\exp(-w/L) - \alpha L\exp(-\alpha L)}{(1-\alpha L)\cosh(w/L)}\right),\ V_{\rm s} = 0, \tag{13}$$

where

$$J_\infty = \frac{q\exp(-x_j\alpha)F_i(1-R)\alpha L}{1+\alpha L},\ V_{\rm s}\to\infty. \tag{14}$$

$F_{\rm i}$ is the incident photon flux, and R is the front surface reflection coefficient. J_∞ is the current density for thick cells (i.e., $w/L \gg 1$).

The number of electrons collected per absorbed photon, $Q_{\rm a}$, where

$$Q_{\rm a} = \frac{J}{qF_{\rm i}(1-R)} \tag{15}$$

is plotted for several values of α in Fig. 1, where Equation (11) is used for J.

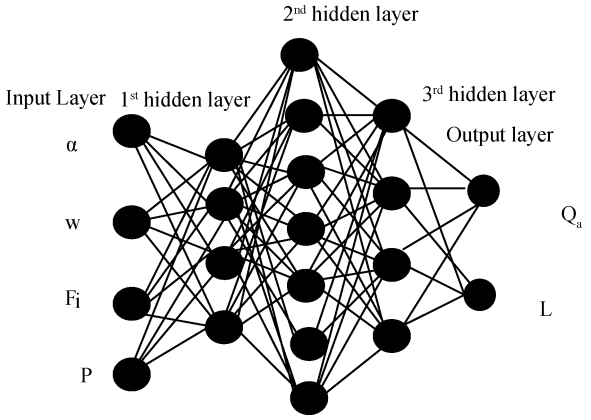

Fig. 2. Optimized neural network.

3. Experimental

A silicon solar cell with an impurity concentration of 10^{15} cm^{-3} or more is considered in the present study.

To obtain a diffusion length measurement by using the injection technique, the required elements are[3,4]:

(1) a source of monochromatic infrared light,

(2) a means of measuring the front surface reflection coefficient,

(3) a determination of the optical power incident on the active cell area,

(4) a measurement of the resulting short-circuit current.

The infrared light was obtained by filtering light from a high-intensity xenon source[5–8]. The filters were Ealing multilayer filters with band-widths of 0.01 μm. The reflection coefficient was measured by using a Gier-Dunkle integrating sphere and a modified Beckman DK-2A spectrophotometer.

The optical power was measured by using a thermopile, while the shot-circuit current was obtained by measuring the voltage across a 1 Ω shunt resistor.

Both measurements were reproducible to within about 0.2%. However, because of uncertainties in the value of the active area, which may vary from one cell to another, the overall accuracy may be reduced.

From these data a value for $Q_{\rm a}$ can be obtained:

$$Q_{\rm a} = \frac{1}{1-R}\ \frac{hc}{qP\lambda}\ \frac{I_{\rm SC}}{A_{\rm a}}, \tag{16}$$

where h is Planck's constant, c is the velocity of light, P is the optical power, $I_{\rm SC}$ is the short-circuit current, λ is the wavelength, and $A_{\rm a}$ is the active area. Then the value of the diffusion length can be obtained from Eqs. (11)–(13).

4. Computing calculation

Using the Matlab package, we could successfully predict the diffusion length taking the values of the cell thickness into account. The Neural network (NN) is a very powerful predictive modeling technique. The initial stage of the program simulation involved data collection and entry (the incident photon flux intensity, the absorption coefficient, the cell thickness, and the optical power) (Fig. 2). In this case, we use the supervised

Table 1. Predicted and measured values of the diffusion length in solar cells (α = 150 cm^{-1}).

Parameter	Measured parameter value using infrared technique	Measured parameter value using photoconductive decay method	Predicted parameter value using a neural network
Diffusion length (μm)	200.1	198.9821	200.07

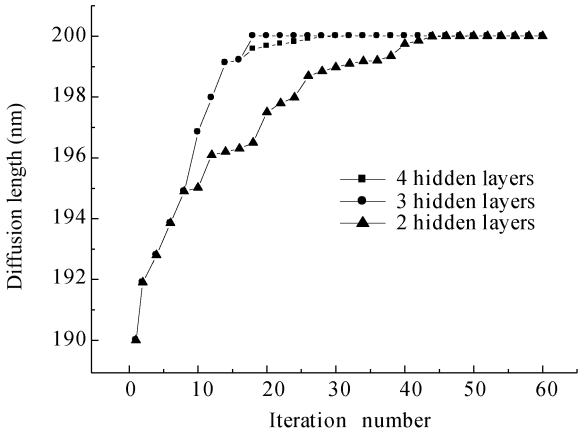

Fig. 3. Computing calculation of the diffusion length for different numbers of neural networks.

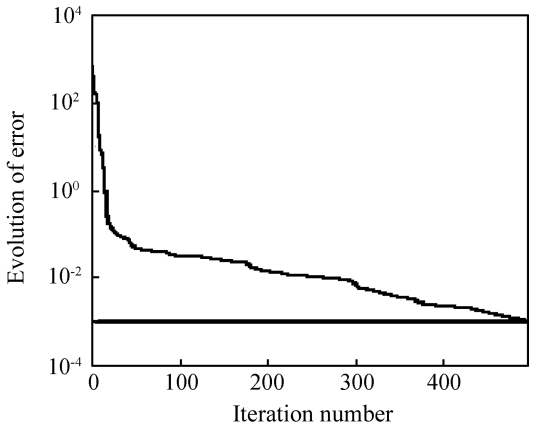

Fig. 4. Error goal convergence.

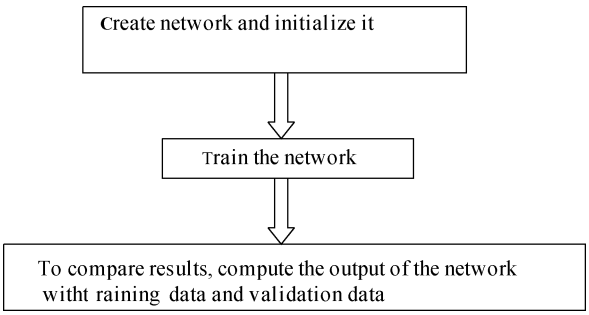

Fig. 5. Basic flow diagram of the ANN.

learning, so a desired output result for each input vector is required when the network is trained; i.e. an ANN (artificial neural network) of the supervised learning type, such as the multilayer perceptron, uses the target result to guide the formation of the neural parameters. It is, thus, possible to make the neural network learn the behavior of the process under study (Fig. 2).

The askew of every layer becomes an additional input of the layer (Fig. 2). Thus, the outputs are calculated by

$$y_j^{(1)} = f\left(\sum_{i=1}^{n_0} w_{ji} + b_j\right) = f\left(\sum_{i=0}^{n_0} w_{ji} x_i\right), \qquad (17)$$

with $x_0 = 1$ and $w_{j0} = b_j$.

*Layer 1: $W_1 = \left[w_{ji}\right]$.

*Layer 2: $W_2 = \left[w_{kj}\right]$.

***Error propagation**

The error expression is given by

$$e_\xi = y_\xi^{\mathrm{d}} - y_\xi = [e_{\xi 1} \cdots e_{\xi \mathrm{n}2}], \qquad (18)$$

where y_ξ^{d}–y_ξ are the desired outputs.

Figure 3 illustrates our computing calculation for different numbers of neural network layers. The convergence to the error goal is shown in Fig. 4. We remark that a faster convergence to the error goal of 0.001 is reached for three hidden layers. The basic flow diagram is shown in Fig. 5

Thus, the predictive errors were measured by the mean error function (MEF) as

$$\mathrm{MEF} = \frac{1}{n}\sum_{i=1}^{n} \frac{|p_i - e_i|}{e_{\max} - e_{\min}} \times 100\%, \qquad (19)$$

where e_i is the experimental value of sample i, p_i is the predicted value of sample i, and n is the number of the samples. $e_{\max}$ and $e_{\min}$ are the maximum and minimum experimental errors value, respectively.

5. Discussion

Theoretical considerations are implemented in a MATLAB 7.1 environment and simulation results are presented for the computational diffusion length.

The results in Table 1 show an excellent agreement with experimental techniques used in measuring diffusion lengths. Perhaps the major factor is the choice of the number of ANN layers. The presented method demonstrates remarkable practical flexibility and efficiency optimization of the convergence. In measuring diffusion lengths using the ANN approach, one can remark that two things are apparent in ANN. With all neural network problems, we face the question of determining the reasonable, if not optimum, size of the network. Let us make the size of the network bigger. This brings in more network parameters, so we have to keep in mind that there are more data points than network parameters. The other thing that could be done is to improve the training algorithm performance or even change the algorithm.

Comparing both experimental techniques, one deduces that each method has its advantages and disadvantages[5]. Previous results can be easily reanalyzed to conclude that the predicted and measured values of diffusion lengths in solar cell (α = 150 cm^{-1}), using infrared technique, are more convergent than the predicted values/measured values by a decay method.

6. Conclusion

In summary, a new computing method of determining the solar cell diffusion length has been proposed. From the results above, it would be justified for a computer program using neural network to be easily adapted for the calculation of solar cell diffusion lengths. Furthermore, the comparative analysis with different experimental techniques shows a good agreement between theoretical calculations and experimental results.

References

[1] Zhu J M, Shen W Z, Zhang Y H, et al. Determination of effective diffusion length and saturation current density in silicon solar cells. Physica B, 2005, 355: 408

[2] Saritas M, McKell H D. Comparison of minority-carrier diffusion length measurements in silicon by the photoconductive decay and surface photovoltage methods. J Appl Phys, 1988, 63: 4561

[3] Sontag D, Hahn G, Geiger P, et al. Two-dimensional resolution of minority carrier diffusion constants in different silicon materials. Solar Energy Materials and Solar Cells, 2002, 72(1–4): 533

[4] Nilsson N G. Determination of carrier lifetime, diffusion length, and surface recombination velocity in semiconductors from photo-excited infrared absorption. Solid-State Electron, 1964, 7(6): 455

[5] Reynolds J H, Meulenberg Jr A. Measurement of diffusion length in solar cells. J Appl Phys, 1974, 45(6): 2582

[6] Belinski J R, Brooks E H, Cocca V, et al. Proton-neutron damage equivalence in Si and Ge semiconductors. IEEE Trans Nucl Sci, 1963, 10(5): 71

[7] Stutenbaeumer U, Lewetegn E. Comparison of minority carrier diffusion length measurements in silicon solar cells by the photo-induced open-circuit voltage decay (OCVD) with different excitation sources. Renewable Energy, 2000, 20(1): 65

[8] Murad J. Improvements in IR photocurrent scanning. Solar Cells, 1990, 28(1): 69